European Radiology (2022) 32:1902–1911
https://doi.org/10.1007/s00330-021-08278-x

CHEST

Differentiating pulmonary metastasis from benign lung nodules in thyroid cancer patients using dual-energy CT parameters

Taeho Ha[1] · Wooil Kim[2] · Jaehyung Cha[3] · Young Hen Lee[1] · Hyung Suk Seo[1] · So Young Park[4] · Nan Hee Kim[4] · Sung Ho Hwang[5] · Hwan Seok Yong[6] · Yu-Whan Oh[5] · Eun-Young Kang[6] · Cherry Kim[1]

Received: 29 March 2021 / Revised: 1 August 2021 / Accepted: 16 August 2021 / Published online: 25 September 2021

Abstract

Objectives To explore the importance of quantitative characteristics of dual-energy CT (DECT) between pulmonary metastasis and benign lung nodules in thyroid cancer.

Methods In this retrospective study, we identified 63 patients from our institution's database with pathologically proven thyroid cancer who underwent DECT to assess pulmonary metastasis. Among these patients, 22 had 55 pulmonary metastases, and 41 had 97 benign nodules. If nodules showed increased iodine uptake on I-131 single-photon emission computed tomography-computed tomography or increased size in follow-up CT, they were considered metastatic. We compared the clinical findings and DECT parameters of both groups and performed a receiver operating characteristic analysis to evaluate the optimal cutoff values of the DECT parameters.

Results Patients with metastases were significantly older than patients with benign nodules ($p = 0.048$). The DECT parameters of the metastatic nodules were significantly higher than those of the benign nodules (iodine concentration [IC], 5.61 ± 2.02 mg/mL vs. 1.61 ± 0.98 mg/mL; normalized IC [NIC], 0.60 ± 0.20 vs. 0.16 ± 0.11; NIC using pulmonary artery [NIC_{PA}], 0.60 ± 0.44 vs. 0.15 ± 0.11; slope of the spectral attenuation curves [λHU], 5.18 ± 2.54 vs. 2.12 ± 1.39; and *Z*-effective value [Z_{eff}], 10.0 ± 0.94 vs. 8.79 ± 0.75; all $p < 0.001$). In the subgroup analysis according to nodule size, all DECT parameters of the metastatic nodules in all subgroups were significantly higher than those of the benign nodules (all $p < 0.05$). The cutoff values for IC, NIC, λHU, NIC_{PA}, and Z_{eff} for diagnosing metastases were 3.10, 0.29, 3.57, 0.28, and 9.34, respectively (all $p < 0.001$).

Conclusions DECT parameters can help to differentiate metastatic and benign lung nodules in thyroid cancer.

Key Points

- *DECT parameters can help to differentiate metastatic and benign lung nodules in patients with thyroid cancer.*
- *DECT parameters showed a significant difference between benign lung nodules and lung metastases, even for nodules with diameters ≥ 3 mm and < 5 mm.*
- *Among the DECT parameters, the highest diagnostic accuracy for differentiating pulmonary metastases from benign lung nodules was achieved with the NIC and IC, followed by the NIC_{PA} and λHU, and their cutoff values were 0.29, 3.10, 0.28, and 3.57, respectively.*

Keywords Thyroid neoplasms · Tomography, X-ray computed · Lung neoplasms · Neoplasm metastasis

✉ Cherry Kim
cherrykim0505@gmail.com

1 Department of Radiology, Ansan Hospital, Korea University College of Medicine, 123, Jeokgeum-ro, Danwon-gu, Ansan-si, Gyeonggi 15355, South Korea

2 Department of Radiology and Medical Imaging, University of Virginia Health System, 1215 Lee St, Box 800170, Charlottesville, VA, USA

3 Medical Science Research Center, Ansan Hospital, Korea University College of Medicine, 123, Jeokgeum-ro, Danwon-gu, Ansan-si, Gyeonggi 15355, South Korea

4 Department of Endocrinology, Ansan Hospital, Korea University College of Medicine, 123, Jeokgeum-ro, Danwon-gu, Ansan-si, Gyeonggi 15355, South Korea

5 Department of Radiology, Anam Hospital, Korea University College of Medicine, 73, Goryeodae-ro, Seongbuk-gu, Seoul 02841, South Korea

6 Department of Radiology, Guro Hospital, Korea University College of Medicine, 148, Gurodong-ro, Guro-gu, Seoul 08308, South Korea

Abbreviations

DECT	Dual-energy CT
IC	Iodine concentration
LN	Lymph node
NIC	Normalized iodine concentration
Tg	Thyroglobulin
TSH	Thyroid-stimulating hormone
VMI	Virtual monochromatic image
Z_{eff}	Z-effective value
λHU	Slope of the spectral attenuation curve

Introduction

Metastasis is correlated with prognosis in differentiated thyroid carcinoma. The lung is the most common site of metastasis [1–6]. Lung metastasis occurs in 33% of patients with medullary thyroid carcinoma [7], and distant metastasis is the main cause of cancer-related death [8]. Distant metastasis in poorly differentiated thyroid carcinoma can cause poor outcomes despite aggressive surgery [9]. Therefore, the diagnosis of lung metastasis is crucial to predicting the prognosis of thyroid cancer.

Dual-energy CT (DECT) has recently re-emerged as an advancement, offering new functional and specific information [10]. This imaging modality can provide virtual monochromatic images (VMI), iodine concentration (IC), slope of the spectral attenuation curves (λHU), and an effective atomic number (Z_{eff}). Several studies have shown significant differences in DECT parameters between malignant and benign lung lesions. Deniffel et al. showed that IC and CT attenuation were useful for differentiating lung metastases of unknown origin [11]. Several studies have shown that DECT parameters, including IC, normalized IC (NIC), and λHU, can help to differentiate between benign nodules and primary lung cancers [12–16]. However, no studies have evaluated DECT parameters to differentiate lung metastases from thyroid cancer from nonspecific inflammatory lung nodules. In clinical practice, distinguishing between benign inflammatory lung nodules and lung metastasis on conventional chest CT during follow-up of patients with thyroid cancer is difficult, especially when the nodules are very small in size.

This study explores the importance of quantitative DECT characteristics in the differential diagnosis between pulmonary metastasis and benign lung nodules in patients with thyroid cancer.

Materials and methods

This retrospective study was approved by our institutional review board. Informed consent was waived (approval number: 2020AS0187).

Patient characteristics

By searching database, we identified 512 consecutive patients with pathologically proven thyroid cancer between January 2016 and July 2020. Of these, 325 underwent DECT at least three times, with an interval of at least 3 months after thyroid cancer surgery, to determine the possibility of lung metastasis. According to our institution's protocol, when chest CT is required after thyroid cancer surgery, the first CT is performed at least 3 months after surgery, the second CT is performed 6 months after the first CT scan, and the third CT is performed 6 months after the second CT scan. The mean follow-up period for all patients was 27.3 ± 9.8 months.

We designated lung nodules that showed increased iodine uptake on I-131 single-photon emission computed tomography-computed tomography (SPECT-CT) or increased size on two follow-up scans (at least 2 mm according to the Fleischner Society guidelines [17]) as pulmonary metastasis. According to previous guidelines, lung metastases generally grow perceptibly within three months [18]. If it was unclear whether a lung nodule was a metastasis or not, a consensus was reached during a conference with thyroid specialists and radiologists based on clinical/radiological/laboratory findings. Lung nodules that suddenly appeared and decreased in size or disappeared without specific treatment on the follow-up CT scans were classified as benign nodules. Two patients underwent surgical excision and had pathologically confirmed pulmonary metastases. Finally, 41 patients with benign lung nodules and 22 patients with lung metastases were included in this study. Figure 1 summarizes the patient selection process.

CT acquisition technique and reconstruction algorithm

The same protocols were applied to the entire study population. All patients were scanned using a Philips IQon 128-slice dual-layer detector spectral CT scanner (Philips Healthcare). For all patients, a body weight-adapted bolus of an intravenous contrast medium (Optiray 350, Mallinckrodt Medical, Inc.) was administered at a rate of 3 mL/s via a 20-gauge cannula into the antecubital vein using a power injector (Stellant, Medrad). The mean body mass index of all patients was 24.6 ± 2.1 (range, 17.8–28.8). No bolus-tracking technique was used, and scanning automatically began 40 s after the administration of the contrast medium. The CT scan parameters were as follows: kVp, 120; 3D dose modulation (DoseRight Index), 20 (reference mAs, 103 mAs); matrix, 512 × 512; scan mode, helical;

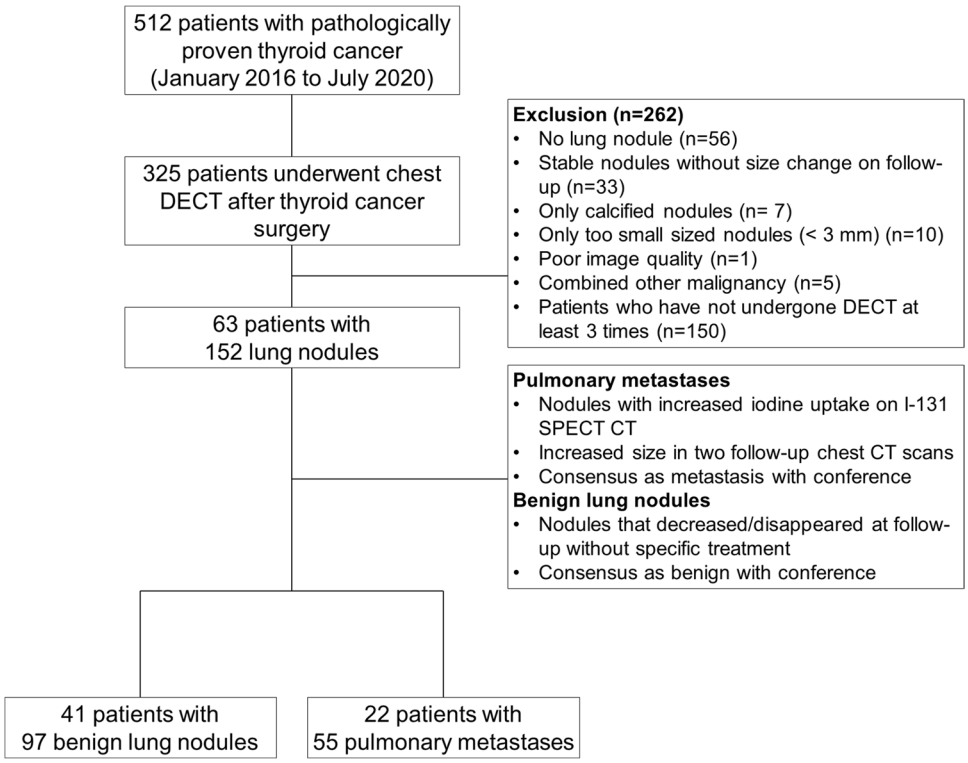

Fig. 1 Summary of the patient selection process. Note: DECT, dual-energy CT

collimation, 64 × 0.625 mm; slice thickness, 1 mm; increment, 0; beam width, 40 mm; focal spot resolution, high; pitch, 0.61; rotation time, 0.4 s; and tube current modulation, 3D modulation. Coronal/sagittal reconstruction was performed using an enhanced scan.

Conventional CT images were reconstructed via hybrid iterative reconstruction (iDose^4, level 3, Philips Healthcare) and a sharp kernel (filter YC). Spectral base images were reconstructed using Spectral (level 3) and a sharp kernel (filter YC) in all patients and contained the conventional CT with the base images. Using spectral base images, VMIs at 40 keV and 100 keV, iodine-based material decomposition, and effective atomic number images were generated.

Image analysis

All images were transferred to ISP (version 10, Philips Healthcare) for evaluation. All DECT parameters were measured by two radiologists with 10 and 3 years of experience in thoracic imaging, respectively (C.K. and T.H.).

The following criteria were applied for lesion selection and DECT parameter measurement to ensure the reliability of the measured DECT values: (1) nodules had a diameter of at least 3 mm. (2) The circular region of interest (ROI) in the lung nodules was placed at the site that best characterized the lesion and was as large as possible. (3) The location of ROI for all measurements was the same. ROI was placed on the conventional image, and the CT number was measured. Then, all of the ROIs were automatically copied onto all VMIs, iodine-based material decomposition, and Z_{eff} images to measure other DECT parameters for the same ROI (Fig. 2). (4) Finally, when multiple lung nodules were present, only three nodules per patient in order of nodule size were included in the analysis. Finally, 55 pulmonary metastases in 22 patients and 97 benign lung nodules in 41 patients were measured.

The IC was measured on the iodine-based material decomposition images. Other ROIs were placed in the descending thoracic aorta at the level of the carina and main pulmonary artery (PA) to obtain the IC of the aorta and PA. To reduce hemodynamic variation in patients, NIC was calculated as follows: NIC = IC of nodule/IC of the aorta, NIC_{PA} was assessed as follows: NIC_{PA} = IC of nodule/IC of PA. The λHU was calculated as follows: λHU = (CT value at 40 keV-CT value at 100 keV)/(100 − 40). The Z_{eff} was automatically calculated by the software. We also evaluated the nodule delineation (well-defined vs. ill-defined) on the conventional image. All values were measured three times and then averaged. The size, delineation, and location of all nodules were also determined and recorded.

Clinical assessment

One radiologist (T. H.) searched electronic medical records. The following clinical data were noted: age, sex, operation type, tumor histologic type, size, multifocality, bilaterality, presence of an extrathyroidal extension, lymphovascular

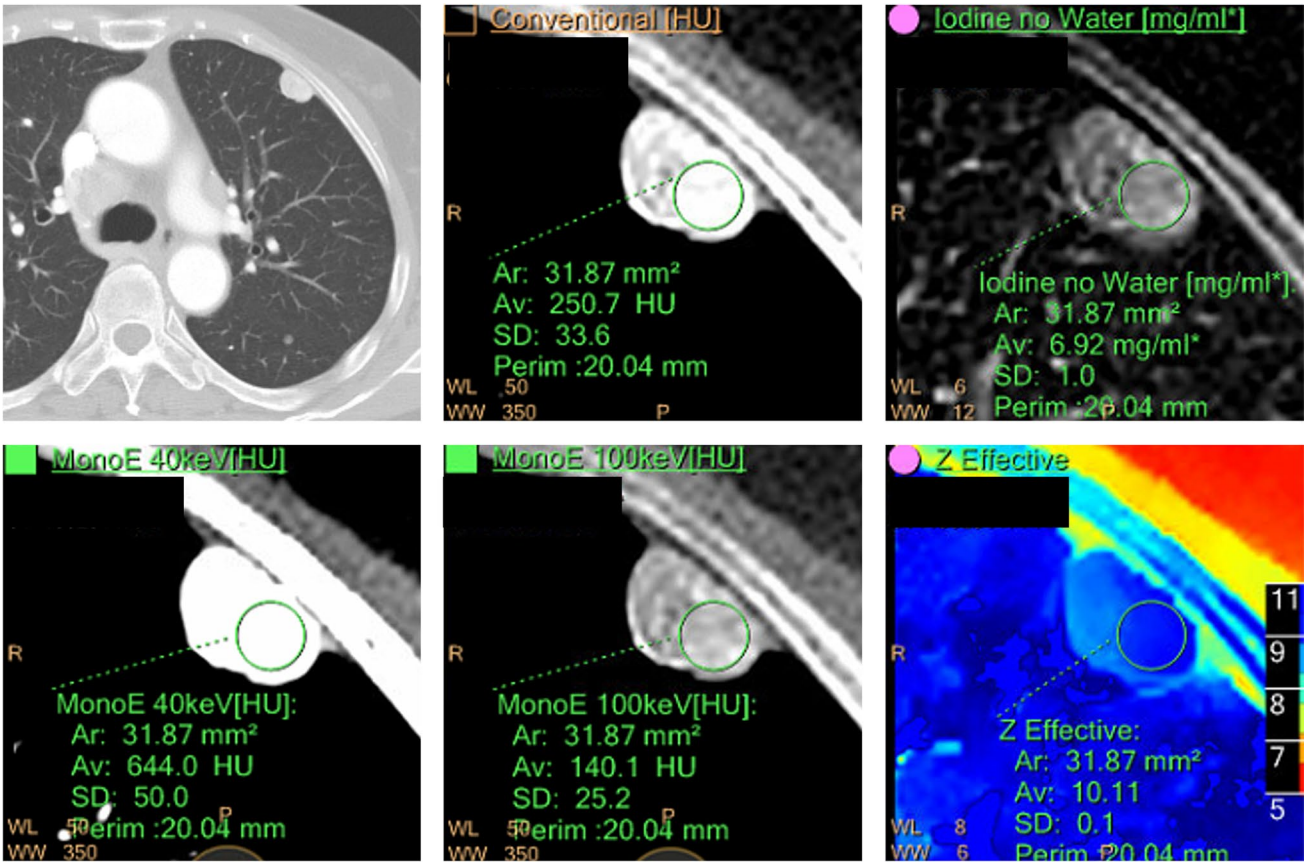

Fig. 2 A 77-year-old woman with a 1.5-cm lung metastasis from papillary thyroid cancer in the left upper lobe. Conventional CT number and dual-energy CT (DECT) parameters including iodine concentration (IC), slope of the spectral attenuation curve (λHU), and Z-effective value (Z_{eff}) were measured with the same region of interest (ROI) at the same location

invasion, number of metastatic lymph nodes (LNs), on thyroglobulin (suppressed Tg), on thyroid-stimulating hormone (suppressed TSH), presence of metastasis in other sites, I-131 activity for lung nodules, I-131 ablation treatment, number of I-131ablation treatments, and cumulative I-131 dose.

Statistical analysis

To compare the clinical findings, nodule size and delineation, CT number, and DECT parameters of the two study populations, chi-square test was used for categorical variables, and Student's *t*-test/Mann–Whitney *U*-test was used for continuous variables. Subgroup analysis was performed according to nodule size (category I: ≥ 3 mm and < 5 mm; category II: ≥ 5 mm and < 7 mm; category III: ≥ 7 mm) to evaluate whether the DECT parameters were significantly different between both groups. DECT parameters of both groups were compared using Mann–Whitney *U*-test. Bonferroni correction was also applied to adjust the *p*-value. A receiver operating characteristic (ROC) analysis was performed, and the area under the ROC curve (AUC) was calculated to assess the diagnostic value of DECT parameters for identifying lung metastases. The cutoff value with the maximum Youden index was chosen as the optimal cutoff value. Intraclass correlation coefficient (ICC) was used to evaluate interobserver variability. These results were interpreted as follows: < 0.40, poor agreement; 0.40–0.59, fair agreement; 0.60–0.74, good agreement; and 0.75–1.00, excellent agreement. Statistical significance was considered at $p < 0.05$. All statistical analyses were performed using the software IBM SPSS Statistics (Version 25; IBM Corp.), R version 4.0.4 (Packages "OptimalCutpoints" and "epiR"; R Foundation for Statistical Computing), and MedCalc (Version 19.2.3; MedCalc Software).

Results

Baseline characteristics

Table 1 summarizes the clinical characteristics. Patients with metastases were significantly older than patients with benign nodules ($p = 0.048$). Papillary carcinoma was the most common histologic type in both groups. The size of the primary thyroid cancer was significantly larger ($p = 0.028$), and extrathyroidal extension and lymphovascular invasion were significantly more

Table 1 Comparison of the clinical characteristics of the study population

	Patients with lung metastases ($n = 22$)	Patients with benign lung nodules ($n = 41$)	p-value
Age (years)	63.6 ± 19.4	55.1 ± 13.8	0.048
Male sex (%)	10 (45.5)	11 (26.8)	0.224
Operation type (%)			0.545
Total thyroidectomy	21 (95.5)	38 (92.7)	
Right/left lobectomy	1 (4.5)	3 (7.3)	
Tumor histology (%)			0.810
Papillary carcinoma	20 (90.9)	38 (92.7)	
Follicular carcinoma	1 (4.5)	2 (4.9)	
Medullary carcinoma	0 (0.0)	1 (2.4)	
Poorly differentiated carcinoma	1 (4.5)	0 (0.0)	
Primary tumor size (cm)	2.8 ± 1.8	1.8 ± 1.3	0.028
Multifocality (%)	9 (50.0)	19 (66.7)	> 0.999
Bilaterality (%)	7 (38.9)	14 (35.9)	> 0.999
Extrathyroidal extension (%)	18 (100.0)	26 (70.3)	0.010
Lymphovascular invasion (%)	6 (75.0)	2 (7.1)	0.002
Number of metastatic lymph nodes	14.1 ± 16.0	7.8 ± 8.9	0.107
Tg (ng/mL)	130.6 ± 415.7	0.9 ± 1.7	< 0.001
TSH (uIU/mL)	7.3 ± 19.8	1.6 ± 4.1	0.372
Other metastasis (%)			0.146
None	19 (79.2)	38 (92.5)	
Bone	1 (4.2)	3 (7.5)	
Pleural	2 (8.3)	0 (0.0)	
Brain	2 (8.3)	0 (0.0)	
I-131 activity (%) ($n = 55$)			0.037
Yes	3 (15.8)	0 (0.0)	
No	16 (84.2)	36 (100.0)	
I-131 ablation treatments (%)	19 (90.5)	35 (89.7)	> 0.999
Number of I-131 ablation treatments (%)	3.4 ± 1.8	1.6 ± 1.1	< 0.001
Cumulative I-131 dose (mCi)	459.3 ± 258.8	204.6 ± 160.0	< 0.001

Tg, thyroglobulin; *TSH*, thyroid-stimulating hormone

common in the metastasis group (all $p < 0.05$). In the laboratory results, the on-Tg level was significantly higher in the metastasis group ($p < 0.001$). Among the four patients who had metastases other than pulmonary metastases, one patient with a benign inflammatory nodule had bone metastasis, and the other three patients with lung metastases had bone/brain, pleural, and pleural/brain metastases, respectively.

The results of the I-131 scan were available for 55 patients. Only three (15.8%) patients with lung metastases showed metabolic uptake of I-131. The patients with lung metastases received significantly more I-131 ablation treatments and had a significantly higher cumulative I-131 doses than the patients with benign lesions (all $p < 0.001$).

Differences in general CT findings

Table 2 and electronic supplementary material eTable 1 show the differences in size, CT number, nodule delineation, and location between benign lung nodules and lung metastasis according to the nodule size categories. The mean size of the pulmonary metastases was significantly larger than that of the benign lung nodules ($p = 0.022$). In the subgroup analysis according to nodule size, benign lung nodules were significantly larger than lung metastases ($p < 0.005$) in category I, and there were no significant differences in nodule size between the two groups in categories II and III.

The CT number of pulmonary metastasis was also significantly higher than the CT number of benign lung nodules ($p < 0.001$). However, there were no significant differences in nodule delineation between the two groups ($p > 0.999$). In the subgroup analysis according to nodule size, the CT number was significantly higher in the lung metastasis than in the benign lung nodules in all categories ($p < 0.01$).

Table 2 Differences in size, CT number, and delineation of nodules between benign lung nodules and lung metastases in thyroid cancer

All nodules	Lung metastasis ($n = 55$)	Benign lung nodules ($n = 97$)	p-value
Size (mm)	6.70 ± 3.34	5.52 ± 2.23	0.022
CT number (HU)	129.01 ± 56.87	59.83 ± 34.09	< 0.001
Delineation			
Well-defined	50 (90.9%)	87 (89.7%)	> 0.999
Ill-defined	5 (9.1%)	10 (10.3%)	
Category I: ≥ *3 mm and* < *5 mm*	Lung metastasis ($n = 17$)	Benign lung nodules ($n = 45$)	p-value
Size (mm)	3.47 ± 0.74	4.08 ± 0.40	0.005
CT number (HU)	122.31 ± 37.74	58.73 ± 28.11	< 0.001
Delineation			
Well-defined	17 (100%)	45 (100%)	N/A
Ill-defined	0	0	
Category II: ≥ *5 mm and* < *7 mm*	Lung metastasis ($n = 17$)	Benign lung nodules ($n = 33$)	p-value
Size (mm)	5.75 ± 0.45	5.49 ± 0.52	0.076
CT number (HU)	121.42 ± 69.16	60.03 ± 39.24	0.003
Delineation			
Well-defined	17 (100%)	33 (100%)	N/A
Ill-defined	0	0	
Category III: ≥ *7 mm*	Lung metastasis ($n = 21$)	Benign lung nodules ($n = 19$)	p-value
Size (mm)	10.09 ± 2.80	9.00 ± 2.78	0.228
CT number (HU)	140.59 ± 59.50	62.08 ± 39.00	< 0.001
Delineation			
Well-defined	16 (76.2%)	9 (47.4%)	0.102
Ill-defined	5 (23.8%)	10 (52.6%)	

DECT, dual-energy CT

Differences between DECT parameters

Table 3 demonstrates the comparison of DECT parameters between benign lung nodules and pulmonary metastases. The IC, NIC, NIC_{PA}, and λHU values were significantly higher in the metastasis group than in the benign group (all $p < 0.001$). There were significant differences in Z_{eff} between the metastasis and benign groups ($p < 0.001$).

In the subgroup analysis according to nodule size, the IC, NIC, NIC_{PA}, λHU, and Z_{eff} of lung metastases were significantly higher than those of the benign lung nodules in all size categories (all $p < 0.05$). Inter-reader reliability was excellent (ICC = 0.889–0.970).

Diagnostic value of CT number and DECT parameters for pulmonary metastasis

The cutoff values, AUCs, accuracy, sensitivity, specificity, positive predictive values, and negative predictive values of the CT number and each DECT parameter are shown in Table 4, Fig. 3, and electronic supplementary material eFigure 1. The AUCs of all DECT parameters ranged from 0.852 to 0.979 (all $p < 0.001$). Among the DECT parameters, the highest diagnostic accuracy for differentiating pulmonary metastasis from benign lung nodules was for NIC and IC, followed by NIC_{PA} and λHU, and their cutoff values were 0.29, 3.10, 0.28, and 3.57, respectively.

Discussion

The present study revealed that the DECT parameters of benign lung nodules and lung metastases from thyroid cancer were significantly different. The cutoff values for each DECT parameter for differentiating lung metastasis from thyroid cancer were also determined. The DECT parameters significantly differed between benign lung nodules and lung metastasis for small nodules, even those measuring ≥ 3 mm and < 5 mm.

As non-functioning metastases have been reported in 10 – 30% of papillary and follicular thyroid carcinoma [19–22], metastatic lesions might lose the ability to take up I-131. Therefore, an I-131 scan cannot be used for diagnostic purposes in these cases [23]. Our study also showed metabolic uptake of I-131 in only 15.8% of patients with lung

Table 3 Differences in DECT parameters between benign lung nodules and lung metastases in thyroid cancer

All nodules	Lung metastasis ($n = 55$)	Benign lung nodules ($n = 97$)	*p*-value
IC (mg/mL)	5.61 ± 2.02	1.61 ± 0.98	< 0.001*
NIC	0.60 ± 0.20	0.16 ± 0.11	< 0.001*
NIC_{PA}	0.60 ± 0.44	0.15 ± 0.11	< 0.001*
λHU	5.18 ± 2.54	2.12 ± 1.39	< 0.001*
Z_{eff}	10.0 ± 0.94	8.79 ± 0.75	< 0.001*
Category I: ≥ *3 mm and* < *5 mm*	Lung metastasis ($n = 17$)	Benign lung nodules ($n = 45$)	*p*-value
IC (mg/mL)	5.88 ± 1.82	1.58 ± 0.78	< 0.001*
NIC	0.55 ± 0.18	0.15 ± 0.08	< 0.001*
NIC_{PA}	0.47 ± 0.16	0.15 ± 0.09	< 0.011*
λHU	4.55 ± 2.09	1.94 ± 1.07	< 0.001*
Z_{eff}	10.25 ± 0.87	8.70 ± 0.72	< 0.001*
Category II: ≥ *5 mm and* < *7 mm*	Lung metastasis ($n = 17$)	Benign lung nodules ($n = 33$)	*p*-value
IC (mg/mL)	5.04 ± 2.11	1.52 ± 0.98	< 0.001*
NIC	0.57 ± 0.18	0.16 ± 0.11	< 0.001*
NIC_{PA}	0.51 ± 0.16	0.15 ± 0.12	< 0.001*
λHU	4.82 ± 2.57	2.29 ± 1.69	0.001*
Z_{eff}	9.57 ± 1.06	8.78 ± 0.79	0.012*
Category III: ≥ *7 mm*	Lung metastasis ($n = 21$)	Benign lung nodules ($n = 19$)	*p*-value
IC (mg/mL)	5.86 ± 2.08	1.82 ± 1.39	< 0.001*
NIC	0.65 ± 0.23	0.19 ± 0.16	< 0.001*
NIC_{PA}	0.77 ± 0.65	0.15 ± 0.13	< 0.001*
λHU	5.98 ± 2.73	2.27 ± 1.51	< 0.001*
Z_{eff}	10.14 ± 0.81	8.68 ± 0.82	< 0.001*

DECT, dual-energy CT; *IC*, iodine concentration; *NIC*, normalized iodine concentration using the IC of aorta; $NIC_{PA,}$ normalized iodine concentration using the IC of pulmonary artery; *λHU*, slope of the spectral attenuation curve; Z_{eff}, Z-effective value

*Significant after adjustment with Bonferroni correction

metastases. Other imaging modalities or serum Tg have been recommended to detect metastases when the I-131 scan is negative [24, 25]. However, non-functioning lung metastasis could be detected earlier using DECT parameters, which do

Table 4 The CT number and DECT parameters for differentiating pulmonary metastasis from benign lung nodules in thyroid cancer

	AUC	*p*-value	Cutoff value	Accuracy (%)	Youden index	Sensitivity (%)	Specificity (%)	PPV (%)	NPV (%)
CT number	0.884 (0.822, 0.930)	< 0.001	84.2	84.2 (77.4, 89.6)	0.674	81.8 (69.1, 90.9)	85.6 (77.0, 91.9)	76.3 (63.4, 86.4)	89.2 (81.1, 94.7)
IC	0.975 (0.936, 0.993)	< 0.001	3.10	93.4 (88.2, 96.8)	0.858	90.9 (80.0, 97.0)	94.8 (88.4, 98.3)	90.9 (80.0, 97.0)	94.8 (88.4, 98.3)
NIC	0.979 (0.942, 0.996)	< 0.001	0.29	93.4 (88.2, 96.8)	0.881	96.4 (87.5, 99.6)	91.8 (84.4, 96.4)	86.9 (75.8, 94.2)	97.8 (92.3, 99.7)
NIC_{PA}	0.966 (0.924, 0.989)	< 0.001	0.28	92.1 (86.6, 95.9)	0.845	92.7 (82.4, 98.0)	91.8 (84.4, 96.4)	86.4 (75.0, 94.0)	95.7 (89.4, 98.8)
λHU	0.865 (0.800, 0.915)	< 0.001	3.57	83.6 (76.7, 89.1)	0.608	69.1 (55.2, 80.9)	91.8 (84.4, 96.4)	82.6 (68.6, 92.2)	84.0 (75.6, 90.4)
Z_{eff}	0.852 (0.785, 0.904)	< 0.001	9.34	80.3 (73.0, 86.3)	0.604	80.0 (67.0, 89.6)	80.4 (71.1, 87.8)	69.8 (57.0, 80.8)	87.6 (79.0, 93.7)

Data in parentheses are 95% confidence intervals; *DECT*, dual-energy CT; *IC*, iodine concentration; *NIC*, normalized iodine concentration using IC of the aorta; $NIC_{PA,}$ normalized iodine concentration using IC of pulmonary artery; *λHU*, slope of the spectral attenuation curve; Z_{eff}, Z-effective value

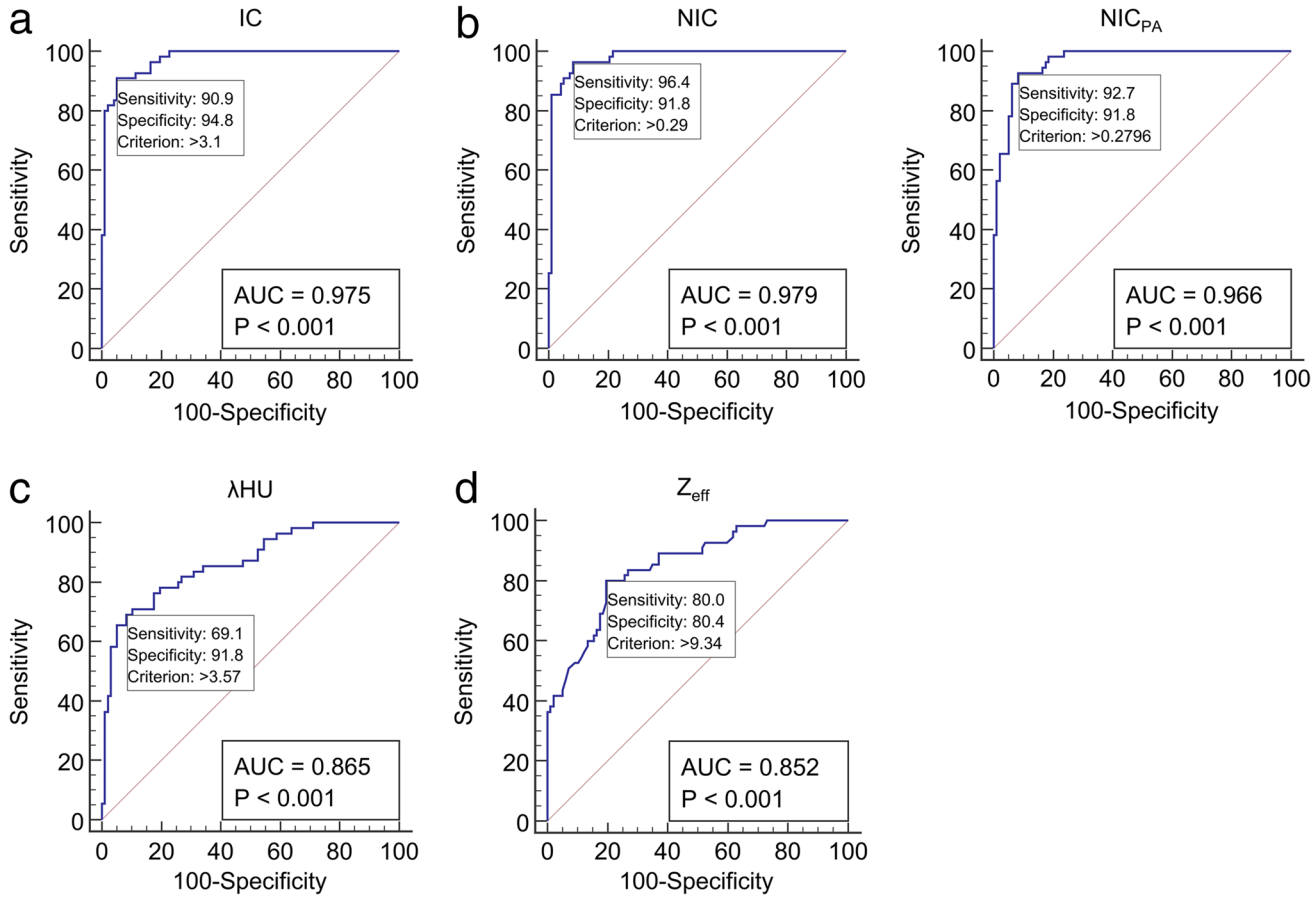

Fig. 3 Receiver operating characteristic curves of dual-energy CT (DECT) parameters for predicting lung metastasis. **a** The iodine concentration (IC), (**b**) normalized IC (NIC) using the IC of the aorta and NIC using IC of the pulmonary artery (NIC_{PA}), (**c**) slope of the spectral attenuation curve, and (**d**) Z-effective value (Z_{eff})

not show I-131 uptake, even in nodules with a diameter of ≥ 3 mm and < 5 mm.

Our results demonstrate that λHU, IC, NIC, and NIC_{PA} of lung metastases from thyroid cancer were significantly higher than the corresponding values of benign lung nodules. Similarly, λHU, IC, and NIC of metastatic LNs of thyroid cancer were also significantly higher than the corresponding values of benign LNs in previous studies [26–28]. Furthermore, a previous study reported that IC was significantly higher in papillary thyroid carcinoma than in benign thyroid nodules [29]. These significantly higher DECT parameters of primary thyroid cancer or metastasis from thyroid cancer might reflect the hypervascularity of primary thyroid cancer because DECT parameters are associated with iodine components and have been shown to reflect microvessel density/blood supply in previous studies [10, 30, 31]. In addition, DECT parameters of thyroid cancer may be the sum of both the blood supply and intrinsic iodine uptake by thyroid tissue [27].

According to previous studies, lung metastases from medullary thyroid carcinoma can contain calcifications as shown on chest CT [32–35]. However, there are no published data for other CT characteristics, particularly the IC of lung metastases in thyroid cancer. Furthermore, although both typically considered hypervascular (e.g., renal cell carcinoma) and hypovascular lung metastases (e.g., colorectal cancer) show similar enhancement patterns on chest CT, Deniffel et al. reported that the IC and NIC of pulmonary metastases differed by primary cancer [11]. Therefore, a quantitative analysis using DECT might be able to differentiate lung metastasis from benign lung nodules in thyroid cancer, despite the similar enhancement patterns.

Lennartz et al. previously reported that there was a considerable data overlap of IC between benign and metastatic lung nodules from various cancers; however, there were significant differences ($p < 0.05$) [36]. There was no significant additional benefit from texture features derived from iodine maps, and only texture analysis-derived features yielded highly accurate differentiation between benign lung nodules and metastatic lung nodules. In contrast, we presented the higher accuracy of DECT parameters than conventional image features (CT number) for differentiating between benign and metastatic lung nodules. These different results might be due to different study populations. The study population in the study by Lennartz et al. was very heterogenous

including at least 12 types of cancers showing both hypervascular and hypovascular features, whereas our study population was very homogeneous and included patients with only thyroid cancer. Therefore, our study could focus on the characteristics of thyroid cancer, which usually demonstrates tumor hypervascularity, and Lennartz et al. had favorable generalizability.

In the present study, there was a significant difference in nodule size between malignant and benign nodules. However, in clinical practice, it is difficult to determine if a nodule is benign or malignant by size alone. We classified the categories by size because the size differed between the two groups and performed subgroup analysis accordingly. In category I, benign nodules were significantly larger than metastases. There were no significant differences in size between both groups in categories II and III. We also suggested cutoff values for DECT parameters. The cutoff value for the NIC was 0.29, and the sensitivity and specificity of this value were 96.4% and 91.8%, respectively, suggesting that it is a reliable value for diagnosing lung metastasis from thyroid cancer. However, further studies with prospective designs are warranted.

In our study, iodine values were normalized using both aorta and PA (NIC and NIC_{PA}). Previous studies presented significant intra-/inter-individual and inter-scan/intrascanner variation in IC [37–39]. Zopfs et al. suggested that normalization of iodine values to the aorta improved reproducibility [38]. In the present study, we performed normalization using the aorta and PA. NIC_{PA} was also a useful DECT parameter for differentiating between benign and metastatic lung nodules from thyroid cancer; however, its accuracy was slightly lower than that of NIC. Research on normalized iodine values using PA is lacking, and further studies on this topic are warranted.

Z_{eff} was significantly higher in lung metastases from thyroid cancer than in benign nodules in our study. Z_{eff} is a quantitative index used to characterize nodule composition and to represent the composite atom for a compound or mixture of various materials; it has a small error rate. However, this index has not been well studied in the field of thoracic oncology [10]. Further study on Z_{eff} in lung metastases from various primary malignancies should be performed before use in clinical practice.

There are several limitations to our study. First, it was a retrospective study performed in a single tertiary hospital. Second, we included patients who were evaluated only with a DECT scanner and excluded those patients who were evaluated with other CT scanners, which may have caused selection bias. In our institution, all CT scans using contrast media in patients with thyroid cancer are performed with a DECT scanner. Unless patients with thyroid cancer require nonenhanced CT due to decreased renal function, most of those who underwent enhanced chest CT were included in this study. Third, only two patients underwent surgical excision for lung metastases and had pathologically confirmed pulmonary metastasis of thyroid cancer. However, in clinical practice, it is hard to obtain tissue for pathologic diagnosis in all patients. Therefore, diagnosis and treatment are performed by combining clinical and imaging findings in real practice. To avoid misclassification between the two groups, the categorization was determined according to established criteria. If those were unclear, a consensus was reached during a conference with thyroid specialists and radiologists based on clinical, radiological, and laboratory findings.

In conclusion, DECT parameters have high diagnostic value for the differential diagnosis of pulmonary metastases from benign lung nodules in patients with thyroid cancer. DECT parameters significantly differed between benign lung nodules and lung metastases even for nodules with diameters of ≥ 3 mm and < 5 mm. These findings may help in the early diagnosis and treatment of pulmonary metastases in patients with thyroid cancer.

Supplementary Information The online version contains supplementary material available at https://doi.org/10.1007/s00330-021-08278-x.

Funding This research was funded by the National Research Foundation of Korea (NRF) (NRF-2018R1D1A1B07049989), Korea University Ansan Hospital research grant (O1903581), and Korea University grant (K2008271).

Declarations

Guarantor The scientific guarantor of this publication is Cherry Kim.

Conflict of interest The authors declare no competing interests.

Statistics and biometry Jaehyung Cha, one of the authors, has contributed to the statistical analysis.

Informed consent Written informed consent was waived by the institutional review board.

Ethical approval Institutional review board approval was obtained.

Methodology
- retrospective.
- case–control study.
- performed at one institution.

References

1. Kim H, Kim HI, Kim SW et al (2018) Prognosis of differentiated thyroid carcinoma with initial distant metastasis: a multicenter study in Korea. Endocrinol Metab (Seoul) 33:287–295
2. Kim M, Kim WG, Park S et al (2017) Initial size of metastatic lesions is best prognostic factor in patients with metastatic differentiated thyroid carcinoma confined to the lung. Thyroid 27:49–58
3. Sabra MM, Ghossein R, Tuttle RM (2016) Time course and predictors of structural disease progression in pulmonary metastases arising from follicular cell-derived thyroid cancer. Thyroid 26:518–524
4. Cho SW, Choi HS, Yeom GJ et al (2014) Long-term prognosis of differentiated thyroid cancer with lung metastasis in Korea and its prognostic factors. Thyroid 24:277–286
5. Hirsch D, Levy S, Tsvetov G et al (2017) Long-term outcomes and prognostic factors in patietns with differentiated thyroid cancer and distant metastases. Endocr Pract 23:1193–1200

6. Shoup M, Stojadinovic A, Nissan A et al (2003) Prognostic indicators of outcomes in patients with distant metastases from differentiated thyroid carcinoma. J Am Coll Surg 197:191–197
7. Giraudet AL, Vanel D, Leboulleux S et al (2007) Imaging medullary thyroid carcinoma with persistent elevated calcitonin levels. J Clin Endocrinol Metab 92:4185–4190
8. Schlumberger M, Bastholt L, Dralle H, Jarzab B, Pacini F, Smit J (2012) 2012 European Thyroid Association guidelines for metastatic medullary thyroid cancer. Eur Thyroid J 1:5–14
9. Ibrahimpasic T, Ghossein R, Carlson DL et al (2013) Poorly differentiated thyroid carcinoma presenting with gross extrathyroidal extension: 1986–2009 Memorial Sloan-Kettering Cancer Center experience. Thyroid 23:997–1002
10. Kim C, Kim W, Park SJ et al (2020) Application of dual-energy spectral computed tomography to thoracic oncology imaging. Korean J Radiol 21:838–850
11. Deniffel D, Sauter A, Dangelmaier J, Fingerle A, Rummeny EJ, Pfeiffer D (2019) Differentiating intrapulmonary metastases from different primary tumors via quantitative dual-energy CT based iodine concentration and conventional CT attenuation. Eur J Radiol 111:6–13
12. Wen Q, Yue Y, Shang J, Lu X, Gao L, Hou Y (2021) The application of dual-layer spectral detector computed tomography in solitary pulmonary nodule identification. Quant Imaging Med Surg 11:521–532
13. Zhang Y, Cheng J, Hua X et al (2016) Can spectral CT imaging improve the differentiation between malignant and benign solitary pulmonary nodules? PLoS One 11:e0147537
14. Chen ML, Li XT, Wei YY, Qi LP, Sun YS (2019) Can spectral computed tomography imaging improve the differentiation between malignant and benign pulmonary lesions manifesting as solitary pure ground glass, mixed ground glass, and solid nodules? Thoracic Cancer 10:234–242
15. Wu L, Cao G, Zhao L et al (2018) Spectral CT analysis of solitary pulmonary nodules for differentiating malignancy from benignancy: the value of iodine concentration spatial distribution difference. Biomed Res Int 2018:4830659
16. Hou WS, Wu HW, Yin Y, Cheng JJ, Zhang Q, Xu JR (2015) Differentiation of lung cancers from inflammatory masses with dual-energy spectral CT imaging. Acad Radiol 22:337–344
17. Bankier AA, MacMahon H, Goo JM, Rubin GD, Schaefer-Prokop CM, Naidich DP (2017) Recommendations for measuring pulmonary nodules at CT: a statement from the Fleischner Society. Radiology 285:584–600
18. MacMahon H, Naidich DP, Goo JM et al (2017) Guidelines for management of incidental pulmonary nodules detected on CT images: from the Fleischner Society 2017. Radiology 284:228–243
19. Casara D, Rubello D, Saladini G et al (1993) Different features of pulmonary metastases in differentiated thyroid cancer: natural history and multivariate statistical analysis of prognostic variables. J Nucl Med 34:1626–1631
20. Degroot LJ, Kaplan EL, McCormick M, Straus FH (1990) Natural history, treatment, and course of papillary thyroid carcinoma. J Clin Endocrinol Metab 71:414–424
21. Thoresen S, Akslen L, Glattre E, Haldorsen T, Lund E, Schoultz M (1989) Survival and prognostic factors in differentiated thyroid cancer–a multivariate analysis of 1,055 cases. Br J Cancer 59:231–235
22. Martin S, Maurice T, Vathaire FD et al (1986) Long-term results of treatment of 283 patients with lung and bone metastases from differentiated thyroid carcinoma. J Clin Endocrinol Metab 63:960–967
23. Küçük NO, Külak HA, Aras G (2006) Clinical importance of technetium-99m-methoxyisobutylisonitrile (MIBI) scintigraphy in differentiated thyroid carcinoma patients with elevated thyroglobulin levels and negative I-131 scanning results. Ann Nucl Med 20:393–397
24. Hung MC, Wu HS, Kao CH, Chen WK, Changlai SP (2003) F18-fluorodeoxyglucose positron emission tomography in detecting metastatic papillary thyroid carcinoma with elevated human serum thyroglobulin levels but negative I-131 whole body scan. Endocr Res 29:169–175
25. Vural GU, Akkas BE, Ercakmak N, Basu S, Alavi A (2012) Prognostic significance of FDG PET/CT on the follow-up of patients of differentiated thyroid carcinoma with negative 131I whole-body scan and elevated thyroglobulin levels: Correlation with clinical and histopathologic characteristics and long-term follow-up data. Clin Nucl Med 37:953–959
26. Liu X, Ouyang D, Li H et al (2015) Papillary thyroid cancer: Dual-energy spectral CT quantitative parameters for preoperative diagnosis of metastasis to the cervical lymph nodes. Radiology 275:167–176
27. Zhao Y, Li X, Li L et al (2017) Preliminary study on the diagnostic value of single-source dual-energy CT in diagnosing cervical lymph node metastasis of thyroid carcinoma. J Thorac Dis 9:4758–4766
28. He M, Lin C, Yin L, Lin Y, Zhang S, Ma M (2019) Value of dual-energy computed tomography for diagnosing cervical lymph node metastasis in patients with papillary thyroid cancer. J Comput Assist Tomogr 43:970–975
29. Gao SY, Zhang XY, Wei W et al (2016) Identification of benign and malignant thyroid nodules by in vivo iodine concentration measurement using single-source dual-energy CT: A retrospective diagnostic accuracy study. Medicine (Baltimore) 95:e4816
30. Wu F, Zhou H, Li F, Wang JT, Ai T (2018) Spectral CT imaging of lung cancer: Quantitative analysis of spectral parameters and their correlation with tumor characteristics. Acad Radiol 25:1398–1404
31. Jia Y, Xiao X, Sun Q, Jiang H (2018) CT spectral parameters and serum tumour markers to differentiate histological types of cancer histology. Clin Radiol 73:1033–1040
32. Seo JB, Im JG, Goo JM, Chung MJ, Kim MY (2001) Atypical pulmonary metastases: spectrum of radiologic findings. Radiographics 21:403–417
33. Hung WW, Wang CS, Tsai KB, Ou-Yang F, Shin SJ, Hsiao PJ (2009) Medullary thyroid carcinoma with poor differentiation and atypical radiographic pattern of metastasis. Pathol Int 59:660–663
34. Jimenez JM, Casey SO, Citron M, Khan A (1995) Calcified pulmonary metastases from medullary carcinoma of the thyroid. Comput Med Imaging Graph 19:325–328
35. Maile CW, Rodan BA, Godwin JD, Chen JT, Ravin CE (1982) Calcification in pulmonary metastases. Br J Radiol 55:108–113
36. Lennartz S, Mager A, Große Hokamp N et al (2021) Texture analysis of iodine maps and conventional images for k-nearest neighbor classification of benign and metastatic lung nodules. Cancer Imaging 21:17
37. Lennartz S, Parakh A, Cao J, Zopfs D, Große Hokamp N, Kambadakone A (2021) Inter-scan and inter-scanner variation of quantitative dual-energy CT: evaluation with three different scanner types. Eur Radiol. https://doi.org/10.1007/s00330-020-07611-0
38. Zopfs D, Reimer RP, Sonnabend K et al (2021) Intraindividual consistency of iodine concentration in dual-energy computed tomography of the chest and abdomen. Invest Radiol 56:181–187
39. Zopfs D, Graffe J, Reimer RP et al (2021) Quantitative distribution of iodinated contrast media in body computed tomography: data from a large reference cohort. Eur Radiol 31:2340–2348